Oscillatory brain activity as unified control mechanism for working memory and mentalizing

Elisabeth V. C. Friedrich[1*], Yannik Hilla[1,2], Elisabeth F. Sterner[1,3], Simon S. Ostermeier[1], Larissa Behnke[1], Paul Sauseng[1*]

[1]Department of Psychology, Research Unit Biological Psychology, Ludwig-Maximilians-University Munich, 80802 Munich, Germany
[2]Allgemeine Psychologie, Universität der Bundeswehr München, 85577 Neubiberg, Germany
[3]Department of Diagnostic and Interventional Neuroradiology, School of Medicine, Technical University of Munich, Munich, Germany

***Corresponding authors:**
paul.sauseng@psy.lmu.de
elisabeth.friedrich@psy.lmu.de

Acknowledgements

We thank Doris Schmid for programming and piloting the experimental design and Daniela Gresch for support with EEG data preprocessing. We are very grateful for the many valuable discussions with Anna Lena Biel and Carola Romberg-Taylor in order to design the experimental tasks. Our special thanks goes to Jörg von Mankowski for providing tools to optimize our experimental design and advice during the complex analyses. We thank Eva Victoria Seegenschmiedt, Nele Habrecht and Ashley Yuan for assisting in designing the social questionnaire and the experimental tasks. This study was funded by a DFG grant to E.V.C.F. (FR 3961/1-1).

Abstract

It has long been thought that coordination of briefly maintained information (so-called working memory) and higher social cognition (mentalizing) rely on mutually exclusive brain mechanisms. However, here we show that slow rhythmical brain activity in the dorsomedial prefrontal cortex controls distributed networks associated with working memory as well as mentalizing during cognitively demanding visual and social tasks. Depending on the effort necessary for cognitive operations, the phase of slow frontal oscillations is used to precisely tune communication with posterior brain areas. For participants having low autistic personality traits, this mechanism is identical across tasks – no matter whether visual or social information is processed. This underpins a unified function of the mentioned oscillatory brain mechanism in working memory and mentalizing. Participants with high autistic personality traits – thus, with difficulty in social cognition – however, have an inability to efficiently tune brain communication depending on cognitive effort in visual information processing. Even more striking, in higher social cognition they fail to implement coordination of distributed brain networks by slow frontal oscillations completely. So, while these findings suggest a unified function of brain oscillations in cognitive coordination they also explain why individuals with high autistic personality traits can have difficulties with demanding cognitive processing across domains.

Keywords: EEG, phase-amplitude coupling, social cognition, autistic traits, theta, gamma

INTRODUCTION

Imagine you are in charge of assigning the best-suited presents to each of your colleagues during the departmental Christmas party. You will need to infer from your colleagues' personality traits which type of present they might like; you will have to hold this information in memory and mentally recombine colleague-present pairings. Depending on how well you do on these complex cognitive operations the Christmas party will result in cheers or awkwardness.

Processing social information, such as what kind of presents someone might like or dislike, strongly relies on activity within a mentalizing network in the brain (Buckner et al., 2008; Frith and Frith, 2006; Schurz et al., 2014; Spunt and Lieberman, 2013; Van Overwalle, 2009). Flexible storage and recombination of information as in the situation described above, however, requires brain activity within a distributed working memory system (Baddeley, 2003; Baddeley et al., 2011; Braver et al., 1997; Cowan, 2008; D'Esposito, 2007; Emch et al., 2019; Miller et al., 2018; Owen et al., 2005; Smith et al., 2017). Until recently it had been believed that there was an antagonistic relationship between activity within the mentalizing and the working memory networks (Anticevic et al., 2010; Fox et al., 2005). Moreover, mentalizing had been investiagted with tasks largely independent of working memory processes (Schurz et al., 2021; Wimmer and Perner, 1983). Meyer and colleagues, however, proposed that really effortful social cognition recruits both fronto-parietal mentalizing and working memory networks (Meyer et al., 2015, 2012; Meyer and Lieberman, 2012). Importantly, a key region in coordinating these effortful social cognitive processes seems to be the dorsomedial prefrontal cortex (Meyer and Collier, 2020).

Brain activity in the Dorsomedial Prefrontal Cortex (DMPFC) can reliably be recorded using electroencephalography (EEG). During cognitively demanding processes this is typically manifested by high amplitude, rhythmical EEG activity over fronto-medial recording sites – the so-called frontal-midline theta activity (FM-theta; Cavanagh and Frank, 2014; Cohen, 2014; de Vries et al., 2020; Sauseng et al., 2019). Recently, it was demonstrated that this FM-theta activity plays a vital role in coordinating distributed cortical networks during demanding working memory processes (Berger et al., 2019; Ratcliffe et al., 2022). Thereby, fast frequency posterior cortical activity (in the gamma frequency range - which can be considered as proxy for working memory activity; Honkanen et al., 2015; Miller et al., 2018; Palva et al., 2010) is nested into specific phases of the FM-theta cycle (Berger et al., 2019). Berger et al. (2019) were able to show that in tasks requiring a lot of cognitive control, posterior gamma activity was nested into FM-theta trough – the excitatory phase. Whereas, when a task was relatively easy, posterior gamma was shifted towards 270° and nested more towards the rather inhibitory peak phase. This way, depending on how effortful a working memory process might be and dependent on how much cognitive control is necessary, fronto-parietal cortical networks can either be coupled or dis-engaged. So, if effortful social cognition requires cooperation between a fronto-parietal mentalizing network and a fronto-parietal working memory network, would those networks be coordinated by the above described FM-theta phase mechanism? And if so, would there be interindividual differences in this mechanism as it is known that there is a large variability in terms of mentalizing skills? Individuals with Autism Spectrum Disorder, for instance, do not only display poor mentalizing abilities (Hamilton and Marsh, 2013; Isaksson et al., 2019; Velikonja et al., 2019) but also difficulties with visual (but not so much verbal) working memory (Barendse et al., 2013; Richmond et al., 2013; Urbain et al., 2015; Wang et al., 2017; Williams et al., 2005, 2014; Xie et al., 2020). They show difficulties in load modulation, need more cognitive effort and show deficits especially in highly demanding tasks (Barendse et al.,

2018, 2013; Rahko et al., 2016; Vogan et al., 2019). Moreover, they show less fronto-parietal network synchronicity (Dichter, 2012; Just et al., 2012; O'Reilly et al., 2017), and autistic traits are correlated with EEG theta activity (Larrain-Valenzuela et al., 2017).
To test our hypotheses, we recorded EEG from two groups of participants – one group with high and one with low autistic-traits while they were doing a social, a visual and a verbal working memory task with two difficulty levels each. We expected that in the social as well as in the visual working memory tasks, fronto-parietal networks would be coordinated by FM-theta phase. We hypothesised that the mechanism of posterior brain activity nesting into different FM-theta phase segments depending on cognitive effort (see Berger et al., 2019) should be observable for the mentalizing network in the same way as for the working memory system. Participants with high autistic-traits were expected to struggle with the social working memory task based on a failure of efficient nesting of posterior high frequency brain activity into the excitatory FM-theta phase. We also hypothesised that participants with high autistic-traits would be more rigid in their dynamic control of fronto-parietal networks in the visual working memory task and would show deficits especially in the highly demanding level of the task. These results should therefore provide strong evidence for a general mechanism of controlling working memory as well as mentalizing networks by the means of FM-theta oscillations. And they should explain why cognitive control in higher social cognition as well as working memory are aberrant in individuals with high autistic-traits.

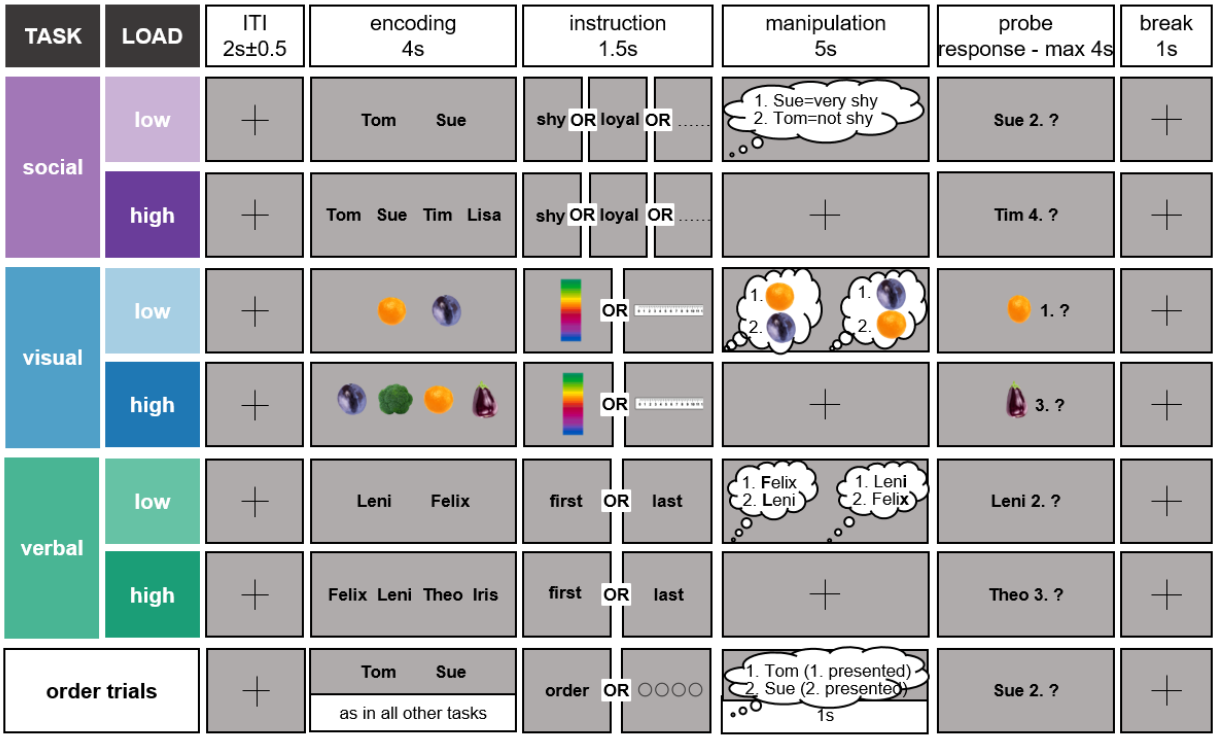

Figure 1. Experimental design. The experiment included three working memory tasks (social, visual and verbal), each implemented in a low and in a high load condition. After an inter-trial interval (ITI) jittered around 2 s (± 0.5 s), either two (low load) or four (high load) stimuli were presented for 4 s, which the participants should encode. In the social task, the displayed names were drawn from the social questionnaire of the screening, in which participants rated their personal contacts according to traits. In the visual task, pictures of fruits and vegetables were displayed and in the verbal task, German names were shown. Then the instruction was displayed for 1.5 s: In the social task, participants should mentally rank their personal contacts according to the displayed trait. In the visual task, the objects

should be mentally sorted either according to color or size. In the verbal task, the names should be alphabetically sorted either according to their first or last letter. In the order trials, participants should remember the stimuli in the same order as they were presented in the encoding period without any manipulation. After the 5-s manipulation period (1-s for order trials), a probe asked whether a specific stimulus was at a specific position in the mental ranking. The participants pressed yes or no as fast and accurate as possible on the left and right mouse key, respectively. Correct and incorrect answers were randomized and occurred equally often. After the response or maximal 4 s, there was a 1-s break before the next trial started.

RESULTS

Behavioral results

In terms of accuracy, participants of both groups achieved a significantly higher performance in the low than high load condition ($F(1, 92)=379.19$, $p<0.001$, partial $\eta^2 = 0.81$). Participants achieved significantly lower accuracies in the social than in the verbal and visual tasks on average ($F(1.67, 153.86)=90.19$, $p<0.001$, partial $\eta^2 = 0.50$). There was also a significant interaction between the tasks and the autistic-traits group ($F(1.67, 153.86)=3.46$, $p=0.042$, partial $\eta^2 = 0.04$): The low autistic-traits group showed a tendency to perform better in the social task (Mdiff=2.15, p=0.15), similar in the visual task (Mdiff=--0.92, p =0.42) and worse in the verbal task (Mdiff=-2.63, p=0.16) than the high autistic-traits group. These differences did not reach statistical significance in the Bonferroni-corrected post-hoc tests.

In terms of reaction time, participants gave their response significantly faster in the low than high load condition ($F(1, 92)=802.17$, $p<0.001$, partial $\eta^2 = 0.9$). Moreover, there was a significant interaction effect between the load conditions and the autistic-traits groups ($F(1, 92)=3.46$, $p=0.035$, partial $\eta^2 = 0.05$): The low and high autistic-traits groups showed similar reaction times in the low load condition (Mdiff=-109.52, p=0.79), whereas the low autistic-traits group showed a tendency to perform faster than the high autistic-traits group in the high load condition (Mdiff=-913.09, p=0.13). Again, these differences did not withhold the significance threshold of the Bonferroni-corrected post-hoc tests. Participants achieved faster reaction times in the social than in the verbal and visual tasks on average ($F(2, 184)=11.17$, $p<0.001$, partial $\eta^2 = 0.11$).

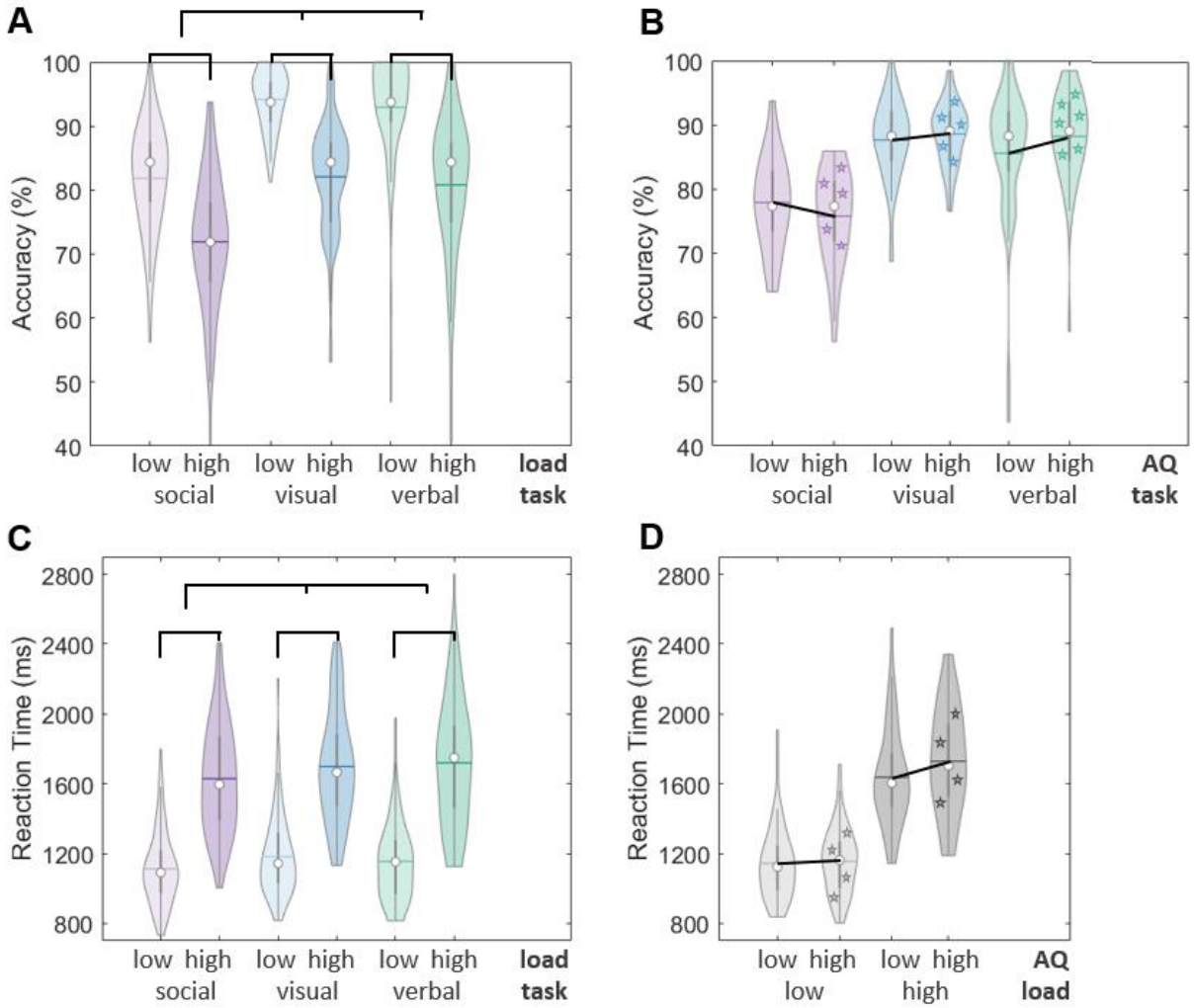

Figure 2. Behavioral results. The data distribution, median (white dot) and mean (colored line) are displayed. **(A)** The low load (light colors) condition showed significantly higher accuracy than the high load (dark colors) condition. The social task (purple) showed significantly lower accuracy than the visual (blue) and verbal (turquoise) tasks. **(B)** There was a significant interaction between tasks and autistic-traits groups (high autistic-traits group indicated with stars) in accuracy. **(C)** The participants showed significantly shorter reaction times in the low load condition than the high load condition. They showed significantly shorter reaction times in the social task than in the visual and verbal tasks. **(D)** There was a significant interaction between low load (light shading) and high load (dark shading) and the autistic-traits groups (high autistic-traits group indicated with stars) in reaction time.

FM-theta phase to posterior gamma amplitude coupling

After EEG pre-processing, we transformed the data into source space based on *a priori* defined regions of interests (ROIs; see supplementary material Table S2) (Meyer et al., 2015, 2012; Meyer and Collier, 2020; Todd and Marois, 2004). Using complex Morlet wavelet transformation, we extracted FM-theta absolute phase values for 4-7 Hz and gamma amplitude between 30-70 Hz in 5 frequency bands. The gamma amplitude of the *a priori* defined posterior ROIs (see Figure 3D) was z-transformed and sorted according to the FM-theta phase segments of the DMPFC. These sorted posterior gamma amplitude values were

used as dependent variable in separate regression models with FM-theta phase segments, load, posterior ROIs and autistic-traits groups as predictor variables to investigate FM-theta phase to posterior gamma amplitude coupling in the different working memory tasks.

Regression models with FM-theta phase segments, load and autistic-traits group as interaction terms reached significance for the social and visual but not the verbal task. That means that FM-theta phase modulated posterior gamma amplitude in the 70-Hz frequency band differently depending on load and autistic-traits in the social (AICc = 34.51) and visual (AICc = 17.66) tasks. Additionally, the same significant interaction effect was observed for the 60-Hz gamma amplitude values in the social task (AICc = 20.84). These effects generalized across posterior ROIs, i.e., regression models with posterior ROIs were not significant. Thus, posterior gamma amplitudes were averaged over posterior ROIs for further analyses.

In order to further explore the significant load modulation in respect to the autistic-traits groups, we fitted our sorted gamma amplitude values to a cosine model. We computed the mean absolute error (MAE; the lower the values the better the fit) in order to determine how well our empirical data fits to a cosine model. This cosine model was then compared (1) to an intercept model to check if the modulation of gamma amplitude was significant over FM-theta phase segments in the respective load condition and autistic-traits group (AIC model comparison cosine vs. intercept, AICc > 2 indicate that the cosine model fits significantly better); and (2) to a null-shift reference cosine model with the peak at 0°/360° and the trough at 180° in order to investigate possible phase shifts.

Social Task

Low autistic-traits individuals' posterior 70-Hz gamma amplitude was periodically modulated by FM-theta phase both under low and high load conditions in the social task. In support of this, their averaged posterior 70-Hz gamma amplitude values barely deviated from the predicted cosine model values as indicated by a very small MAE ($MAE_{Low\ Load}$ = 1.67; $MAE_{High\ Load}$ = 2.40). Moreover, their data fit better to a cosine than an intercept model ($AICc_{Low\ Load}$ =6.11; $AICC_{High\ Load}$ =15.16). In the low load condition, there was a significant phase shift of about 53.57° (CI = [27.57°, 79.57°]) towards 270°. In the high load condition, there was no significant phase shift (CI = [-2.37°; 28.57°]), the maximal gamma amplitude was locked to the FM-theta trough (180°).

In contrast, the model fit of the high autistic-traits individuals' 70-Hz gamma amplitude to the cosine model was worse than the one of the low autistic-traits group ($MAE_{Low\ Load}$ = 5.17; $MAE_{High\ Load}$ = 5.84). In the low load condition, the high autistic-traits individuals' data fit better to the intercept model ($AICc_{Low\ Load}$ = 4.88), suggesting no significant periodically modulation of posterior gamma amplitude by FM-theta. In the high load condition, posterior gamma amplitude was periodically modulated ($AICc_{High\ Load}$ = 8.88). However, their peak gamma amplitude was significantly shifted by on average 37.39° (CI = [-59.40°, -15.38°]) towards 90°, which is in contrast to the low autistic-traits group and our assumed coupling mechanism (Berger et al., 2019).

In the 60-Hz frequency band in the social task, the phase-amplitude coupling was similar but weaker than in the above described 70-Hz frequency band (see supplementary material, Figure S2).

Visual Task

Likewise, low autistic-traits individuals' posterior 70-Hz gamma amplitude in the visual task was periodically modulated both in the low ($MAE_{Low\ Load}$ = 2.17; $AICc_{Low\ Load}$ =10.68) and high load condition ($MAE_{High\ Load}$ = 2.40; $AICc_{High\ Load}$ =14.68). Their peak gamma activity was significantly shifted by on average 57.39° ($CI_{Low\ Load}$ = [37.54°, 77.20°]) towards 270° in the low load condition and locked in the FM-theta trough (180°) in the high load condition (i.e., no significant phase shift, $CI_{High\ Load}$ = [-23.18°; 8.58°]).

Also high autistic-traits individuals' posterior 70 Hz gamma amplitude was periodically modulated by FM-theta phase both in low ($MAE_{Low\ Load}$ = 1.61; $AICc_{Low\ Load}$ =11.28) and high load conditions ($MAE_{High\ Load}$ = 4.12; $AICc_{High\ Load}$ =17.25). However, there was no significant phase shift in the low load condition (CI = [-9.89°, 28.45°]), the highest gamma amplitude was locked in the trough of FM-theta phase (180°). In the high load condition, there was a minimal phase shift of 23.30° (CI = [9.47°, 37.11°]) towards 270°.

Circular-linear correlations between preferred FM-theta phase and autistic traits

For the significant phase-amplitude coupling results, we calculated circular-linear correlations between the preferred FM-theta phase (i.e., phase segment of FM-theta with the highest gamma amplitude) and AQ scores for the subscales over all participants as well as performance. We found a significant correlation between the preferred FM-theta phase based on the 60-Hz frequency band in the social task and the AQ subscales: The preferred FM-theta phase was correlated with imagination in the low load condition (r= 0.30; p= 0.014) and with social skills in the high load condition (r= 0.26; p= 0.036) of the social task.

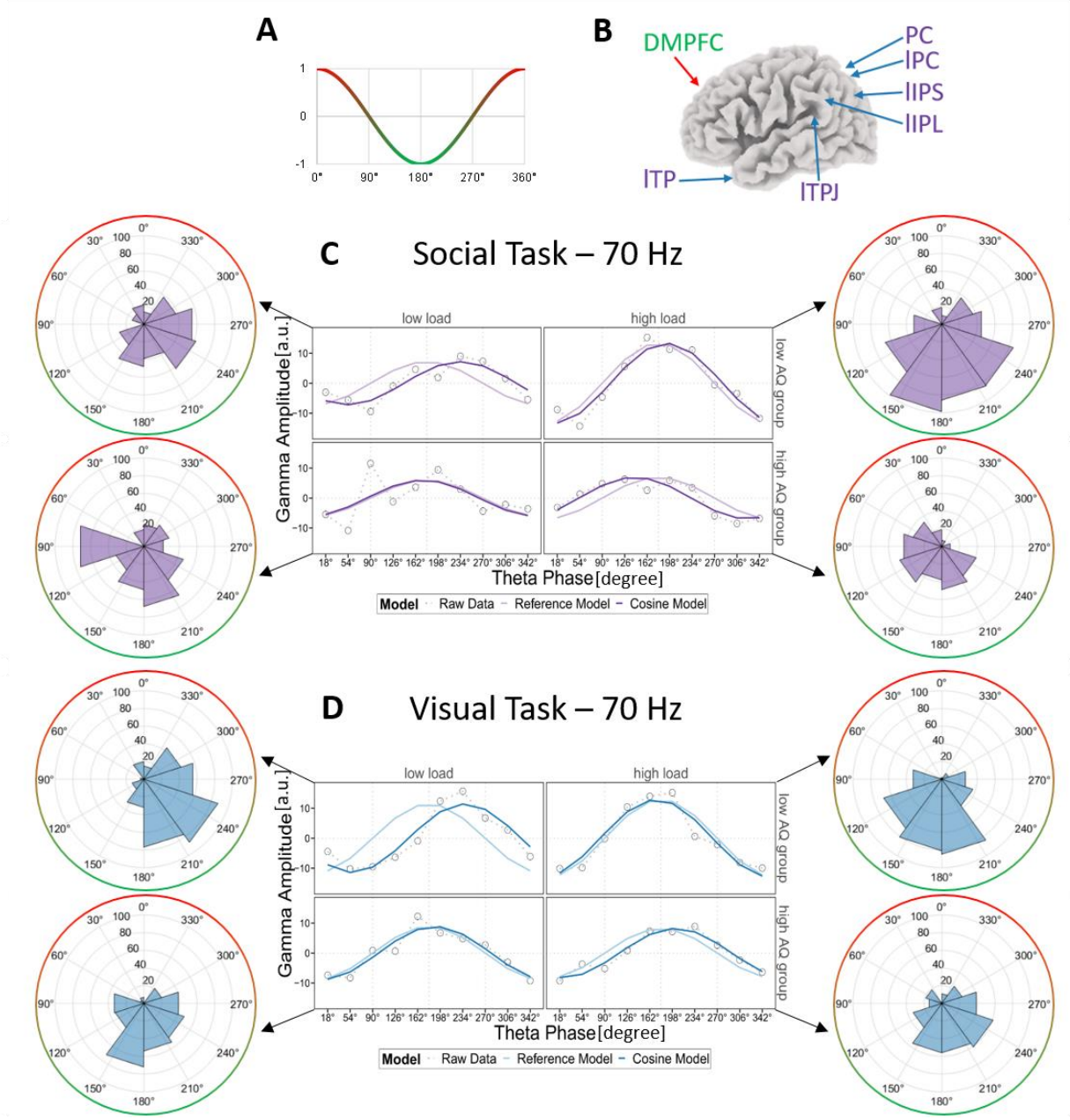

Figure 3: Phase-amplitude coupling. (A) Our cosine model for the FM-theta phase is displayed. The FM-theta trough is at 180° (green color) and FM-theta peak is at 0°/360° (red color). **(B)** FM-theta phase was extracted from the Dorsomedial Prefrontal Cortex (DMPFC; in green/red colors). Posterior gamma amplitude (in purple/blue colors) was extracted from the following 11 posterior regions of interest (ROIs): left and right Temporal Pole (lTP, rTP), left and right Temporo-Parietal Junction (lTPJ, rTPJ), left and right Inferior Parietal Lobe (lIPL, rIPL), left and right Intraparietal Sulcus (lIPS, rIPS), left and right Precuneus/Posterior Cingulate Cortex (lPC, rPC) and medial Precuneus/Posterior Cingulate Cortex (PC). The left and medial ROIs are indicated in the figure, for the exact coordinates of all ROIs, please refer to the supplementary material, Table S2. The z-transformed posterior instantaneous gamma amplitude was sorted according to the FM-theta phase segments and averaged over all 11 posterior ROIs (as there was no significant interaction effect between ROIs and FM-theta phase segments) for analysis and displays (C) and (D) of this figure. **(C)** and **(D)** The sorted z-transformed posterior gamma amplitude of the 70-Hz frequency band is shown in relation to FM-theta phase segments of the DMPFC in the social (purple) and visual (blue) tasks separately for the load conditions and autistic-traits groups. In the circular plots, FM-

theta peak (0°) was indicated in red and FM-theta trough (180°) in green. In the line charts, the grey dots indicate our empirical posterior gamma amplitudes, the light purple or blue lines our cosine reference model (if gamma peak amplitudes were locked in the trough of FM-theta phase) and the dark purple or blue lines the cosine model fitted to our empirical data. In the **(C)** social and **(D)** visual tasks in the low autistic-traits group, the highest gamma amplitudes were locked in the FM-theta trough (180°) in the high load condition and shifted towards 270° in the low load condition. In the **(C)** social task in the high autistic-traits group, there was no significant phase-amplitude coupling in the low load condition and a phase shift towards 90° in the high load condition. In the **(D)** visual task in the high autistic-traits group, the highest gamma amplitudes were locked in the FM-theta trough (180°) already in the low load condition and slightly shifted in the high load condition.

DISCUSSION

We used FM-theta phase to posterior gamma amplitude coupling as a signature of interregional neural coordination. We replicated load-dependent phase-amplitude coupling in a visual working memory task (Berger et al., 2019) and confirmed our hypothesis that the phase-amplitude coupling mechanism can be extended to the social domain in the low autistic-traits group. Specifically, posterior high frequency bursts were locked close to the trough of the FM-theta cycle in the high load and shifted towards 270° of the FM-theta cycle in the low load condition in the social and visual tasks. In contrast, individuals with high autistic-traits displayed a different pattern: In the visual task, posterior gamma amplitude was locked in the FM-theta trough already in the low load condition and slightly shifted in the high load condition. In the social task, we could not find significant phase-amplitude coupling in the low load condition and it was shifted towards 90° in the high load condition. Circular-linear correlations indicated an association between preferred FM-theta phase in the social task and extend of autistic traits. In contrast to the social and visual tasks, this phase-amplitude coupling was not seen in the verbal task.

Behavioral data

Behaviorally, we could confirm our hypothesis that performance was better and faster in the low than high load condition across tasks and autistic-traits groups. The social task achieved significantly worse accuracy (as in Meyer et al., 2015) but faster reaction times (as in Meyer et al., 2020) than the non-social tasks. It seems that a different response strategy led to an accuracy-reaction time trade-off in the social task. Moreover, the criteria for accuracy in the social task (based on the social questionnaire in the screening) was not as reliable as in the visual and verbal tasks. The re-test reliability of the social questionnaire was on average 0.74 and comparable between autistic-traits groups.

Importantly, we also found interactions involving the autistic-traits groups. Compared to the low autistic-traits group, the high autistic-traits group responded equally fast in the low load but showed a tendency to respond slower in the high load condition. This indicates that high autistic-traits individuals can employ compensating mechanisms to achieve comparable behavioral performance in working memory tasks (Audrain et al., 2020; Koshino et al., 2008; Urbain et al., 2015; Yuk et al., 2020). However, in high load conditions, this strategy reaches its limits (Barendse et al., 2018, 2013).

Concerning the tasks, the high autistic-traits group showed a tendency to perform worse in the social task, similar in the visual task and better in the verbal task than the low autistic-traits group. This is in line with autistic-traits and Autism Spectrum Disorder being related to

deficits in mentalizing and reasoning about others (Hamilton and Marsh, 2013; Isaksson et al., 2019; Velikonja et al., 2019) and in visuo-spatial rather than verbal working memory tasks (Barendse et al., 2013; Richmond et al., 2013; Urbain et al., 2015; Wang et al., 2017; Williams et al., 2005, 2014; Xie et al., 2020).

It is important, however, to keep in mind that we did not compare individuals with Autism Spectrum Disorder to neuro-typical controls in this study. Our participants did not show clinically significant disorders that significantly affect their functioning in daily-life. Our two groups did not differ in age, gender, education or intelligence, only in their personality traits, especially in the extend of autistic-traits. Thus, confounding variables were controlled and differences between the groups can be directly ascribed to the extent of autistic traits.

Load-dependent phase-amplitude coupling in the low autistic-traits group

Our phase-amplitude coupling findings in the low autistic-traits group in the visual task replicated the results of Berger et al. (2019). This shows that FM-theta activity generally plays a vital role in coordinating distributed cortical networks during visual working memory processes and is not restricted to a specific task. Moreover, this neural mechanism of neural coordination could be extended to social working memory tasks, showing that FM-theta does not only control the fronto-parietal working memory system but also the mentalizing network. As expected, the DMPFC seems to be the core region for both systems, leading to the proposition of shared neural correlates between the visual and social tasks (Berger et al., 2019; Ferrari et al., 2016; Meyer et al., 2015; Meyer and Collier, 2020; Mottaghy et al., 2002; Schurz et al., 2014; Van Overwalle, 2011).

In contrast, the verbal task did not show the same phase-amplitude coupling. The verbal working memory task might rely rather on the left Dorsomedial Prefrontal Cortex (DLPFC) (Meyer et al., 2015), which was associated with general working memory functions across verbal, visual, social and emotional working memory tasks (Barbey et al., 2013; Braver et al., 1997; D'Esposito, 2007; Meyer et al., 2015; Mottaghy et al., 2002; Mull and Seyal, 2001; Osaka et al., 2007; Owen et al., 2005; Smith et al., 2017). Thus, we analyzed our data with exactly the same procedure but used the left DLPFC instead of the DMPFC for theta phase extraction (see supplementary material, Table S3). Regression models with theta phase segments from the left DLPFC, load and autistic-traits group as interaction terms reached significance for 50-Hz posterior gamma amplitude in the verbal and visual (but not in the social) tasks. However, our phase-amplitude coupling seen in the DMPFC for low autistic-traits individuals could not be confirmed in the left DLPFC (see supplementary material, Figure S3 and S4).

We found a unified system coordinating both mentalizing and working memory processes: FM-theta from the DMPFC coupled and decoupled posterior regions independently of whether they were rather considered as part of the working memory or mentalizing network, incorporating effortful social cognition and demanding visual working memory tasks.

Load-dependent phase-amplitude coupling in the high autistic-traits group

In contrast to the low autistic-traits group (who disengaged the fronto-parietal network in the low load visual task), the high autistic-traits group coupled the fronto-parietal network in the low load condition of the visual task (i.e., highest gamma amplitude was nested in the FM-theta trough). This indicates that high autistic-traits participants needed more cognitive effort to achieve comparable performance as the low autistic-traits group (Audrain et al., 2020; Koshino et al., 2008; Urbain et al., 2015; Yuk et al., 2020). In the high load condition in the visual task, highest posterior gamma amplitudes were also nested around the FM-theta

trough, but slightly shifted towards 270°. This might indicate that the compensating mechanisms reached its limit in the high load condition (Barendse et al., 2018, 2013; Rahko et al., 2016) and the engagement of the fronto-parietal network did not work efficiently anymore. Our assumptions are also in line with our behavioral data, showing similar reaction times in the low load but longer reaction times in the high load condition for high autistic-traits in comparison to low autistic-traits participants. Our results might not only be explained by more effort needed but also by a deficit in load modulation per se (Vogan et al., 2019, 2018, 2014). Individuals with high autistic-traits might be stuck in the effortful mode and unable to efficiently decouple the fronto-parietal network in the low load condition.

In the social task, high autistic-traits individuals failed to show an efficient coupling or decoupling of the fronto-parietal network. In the low load condition, they did not show significant gamma modulation via FM-theta phase. In the high load condition, the highest gamma amplitudes were not nested in the FM-theta trough but shifted towards 90°. A shift towards 90° (in contrast to a shift towards 270° as expected based on Berger et al., 2019), might point to a reverse flow of information in the fronto-parietal network. These findings are in line with studies showing that individuals with Autism Spectrum Disorder display lower activity in the prefrontal cortex and dysfunctions in long-rang connectivity, especially a frontal-posterior underconnectivity in lower frequencies (Dichter, 2012; Just et al., 2012; O'Reilly et al., 2017).

Correlation between the preferred FM-theta phase in the social task and the autistic-traits

Associations between the theta rhythm and autistic-traits were reported in literature (Hill et al., 2022; Larrain-Valenzuela et al., 2017). In our study, the preferred FM-theta phase in the social task was correlated with the AQ subscale imagination in the low load condition and with the AQ subscale social skills in the high load condition. These correlations demonstrate that the phase-amplitude coupling is functional relevant for imagination and social skills, both important aspects of our daily-life and most interesting for mental disorders (Fusar-Poli et al., 2020; Pearson, 2019).

Conclusion

We could show that FM-theta over the DMPFC coordinates the mentalizing network as well as the working memory system by dynamically nesting posterior brain activity into different FM-theta phase segments in relation to load in effortful social and visual working memory tasks. While the visual and social working memory tasks share this neural mechanism, the verbal domain seems to involve different systems.

Moreover, we could show that interindividual differences in autistic traits influenced the efficient coupling and decoupling of fronto-parietal regions in both networks, the mentalizing and working memory system. The load-dependent and dynamic allocation of resources seen in the low autistic-traits group became stuck in the high effort mode in the visual task and failed entirely in the social task in individuals with high autsitic-traits. This phase-amplitude coupling mechanism seems to be functionally relevant and could explain deficits in mentalizing and visual working memory in individuals with high autistic-traits.

Importantly, the found differences in phase-amplitude coupling and behavior are based on mostly subclinical individuals. As Autism is a spectrum disorder, it is hard to set a clean cut-off between neuro-typical individuals and individuals with a disorder. This study included a wide range of participants in respect to the Autism spectrum, who only differed in the extend of autistic traits. Future studies shoud take the deveolpmental component into account (Vogan et al., 2019). This phase-amplitude mechanism might serve as an early predictor for aberrant development. Moreover, it might also help to understand deficits in other mental disorders such as schizophrenia better (Griesmayr et al., 2014).

This FM-theta phase to posterior gamma amplitude coupling might be able to generally explain how resource allocation is coordinated in the brain and why some individuals have problems in some specific tasks and difficult loads.

METHODS

Sample size

We used an *a priori* power analysis to determine the appropriate sample size (MorePower 6.0.4, Campbell and Thompson, 2012). The behavioral effects in load modulation in the social and verbal working memory task in Meyer et al. (2015) reached effect sizes of $\eta^2 \geq 0.19$ for reaction time and $\eta^2 \geq 0.08$ for accuracy. The EEG-based phase-amplitude coupling effects in the visual working memory task in Berger et al. (2019) yielded effect sizes of about partial $\eta^2 = 0.1$. We calculated our sample size for a task x load repeated-measures ANOVA with autistic-traits group as between-subject factor using an alpha level of 0.05, statistical power of 0.9 and a more conservative effect size of partial $\eta^2 = 0.07$. A total sample size of 88 was suggested (i.e., 44 per autistic-traits group). As we expected the exclusion of about 15% of participants due to EEG artifacts or problems with the task, we recorded data of 100 participants, divided into two groups.

Screening

Participants were either assigned to the low or to the high autistic-traits group according to their Autism Spectrum Quotient (AQ; Baron-Cohen et al., 2001). It assesses social skills, attention switching, attention to detail, communication and imagination in five subscales. The scale is sensitive enough to measure autistic traits in the nonclinical population and correlates with social and visual cognitive performance and neurophysiological measures (Baron-Cohen et al., 2001; Gebauer et al., 2015; Richmond et al., 2013; Sevgi et al., 2016). The AQ ranges from 0-50 points, where scores above 32 indicate that individuals have clinically significant levels of autistic traits (Baron-Cohen et al., 2001). We chose a cut-off of 20 to discriminate between sub-clinical individuals with low and high autistic traits because (1) control participants typically scored a mean below 20 (Baron-Cohen et al., 2001; Freitag et al., 2007; Lau et al., 2016; Mealey et al., 2014; Richmond et al., 2013; Sumiyoshi et al., 2011); and (2) individuals with autistic tendencies (e.g., relatives of individuals with ASD or specialists in mathematics) typically scored a mean above 20 (Baron-Cohen et al., 2001; Lau et al., 2016; Sumiyoshi et al., 2011).

Additionally to the AQ, all participants underwent a two-step screening process. In the first step, we asked about sociodemographic data and performed a neuropsychiatric telephone interview to only include participants who showed no clinically significant neurological or psychiatric disorder. We included individuals with scores above 32 on the AQ or a diagnosis of Autism Spectrum Disorder as long as participants were not significantly impaired in their daily-life functioning. The second step was an in-person screening which took place on average 14 days prior to the EEG recording. Statements about handedness and color vision were confirmed based on the short form of the Edinburgh Handedness Inventory (Oldfield, 1971), and with the Ishihara color test, respectively. Verbal intelligence was assessed with the Multiple Choice Vocabulary Test (MWT-B; (Lehrl et al., 1995)). To estimate visuospatial problem solving, the Culture Fair Intelligence Test (CFT 20-R, Scale 2) was used (Cattell and Cattell, 1960). Additionally, the German short version of the Big Five Inventory (BFI-K) was applied to evaluate the Big Five personality traits (Rammstedt and John, 2005).

Finally, participants filled out the social questionnaire based on the experimental design of Meyer and colleagues (Meyer et al., 2015, 2012; Meyer and Lieberman, 2016). Participants indicated 10 personal contacts and evaluated them on 48 German traits on a 1-

100 rating scale in intervals of 5 points (Dumas et al., 2002; Grühn and Smith, 2008). Personal contacts which were ranked ≥ 15 points apart from one another for a specific trait were used to create trials for the social task in the later EEG experiment.

Participants

Of the 100 volunteers, 51 belonged to the low autistic-traits group (AQ ≤ 20) and 49 to the high autistic-traits group (AQ > 20). Both groups included about half male and half female participants who were on average 24 years old (range between 18-39 years). All volunteers had at least a secondary school diploma, German as their native language, were right-handed and had normal or corrected-to-normal vision. None of them was pregnant or had any clinically significant neurological or psychiatric disorder that led to significant impairment in daily-life functioning. Three participants met the criteria for Autism Spectrum Disorder, please see Table S1 in the supplementary material for more information about the participants. There was no difference between the autistic-traits groups in respect to their verbal and non-verbal intelligence scores (CFT 20-R: M_{lowAQ}=114.27, SD_{lowAQ}=13.14, M_{highAQ}=118.45, SD_{highAQ}=13.18, t(98)=-1.58, p=0.12; MWT: M_{lowAQ}=103.71, SD_{lowAQ}=11.49, M_{highAQ}=106.08, SD_{highAQ}=9.83, t(98)=-1.11, p=0.27). Participants were mainly recruited within students of the LMU Munich and Technical University of Munich and were compensated with course credit or 10 € per hour. All participants gave written informed consent prior to participation in the study, which was approved by the LMU Munich Faculty 11 ethics committee.

Experimental design

The experimental design included three different tasks that targeted either social, visual or verbal working memory. The three tasks were implemented in a low and a high load condition. In the low load condition, two stimuli (i.e., two names or two objects) and in the high load condition, four stimuli had to be encoded and manipulated. All tasks relied on the same temporal structure of a trial (Figure 1).

In the social task, the names of the personal contacts - which were indicated in the social questionnaire during the screening process - were used as stimuli. After encoding the names, a trait was presented (e.g., shy), which was also drawn from the social questionnaire. During the manipulation period, participants mentally ranked their contacts according to the trait (i.e., how much the trait applies to the person). Names and traits varied between trials. The probe then asked if a certain name was at a certain position in the mental ranking (e.g. Is Sue second shiest?). For example, the participant should press “no” if Sue was the shiest person (see Figure 1).

In the visual task, the stimuli consisted of 16 pictures of different fruits and vegetables, which naturally vary in color and size. Note that the stimuli were always presented in the same size, which was ensured by using the same amount of colored pixels to depict the objects against the grey background. The instruction was to sort the objects either with respect to color (from green to blue) or with respect to their natural size (from small to large). Both manipulation conditions appeared randomized and equally often. To ensure that participants rely on the same ranking of color and size, a uniform ranking was included in the preparation material (see Procedure) and was rehearsed before the beginning of the EEG experiment.

In the verbal task, names were used as stimuli. The names were drawn randomly from a pool of 16 German names, which all differed in their first and last letter. They were half female and half male names, consisted of 4-6 letters and had no ambiguity how to spell them in respect to their first and last letter. Participants should either sort the names in alphabetical order with respect to their first or last letter. Both manipulation conditions appeared randomized and equally often.

Each task and load condition was presented in a separate block of 16 task-specific trials. We also added 4 order trials to each block (Figure 1). Here, the encoding period was the same as for the task-specific trials (e.g., names as stimuli for the social and verbal task or a picture of an object for the visual task). Instead of the task-specific instruction, participants should remember the stimuli in the presented order without any manipulation. The probe then referred to the original position of the stimulus during the encoding period. The order trials should ensure that participants encoded all stimuli in the presented order and did not start to rank the stimuli before the manipulation period started. The order trials were not analyzed.

Thus, each block included 20 different trials (16 task-specific and 4 order trials) presented in randomized order and lasted for maximal 5.57 minutes depending on the reaction times. Every block was presented twice in randomized order during the whole EEG session, which lasted maximal 66.8 minutes (without breaks between the blocks). From the 240 recorded trials, we recorded 32 task-specific trials per task and load condition.

Procedure and Electrophysiological Recording

After a successful screening, participants were invited to the EEG session. Two days prior to the EEG session, participants were provided with the preparation material, which they had to study. The material included a description of the 48 traits – which was also shown to the participants during the online survey- and the ranking of fruits and vegetables according to color and size. This was to ensure that participants made their choices in the EEG study based on the same definitions and rankings.

In the EEG session, participants sat in a comfortable chair in front of a computer screen. They were provided with detailed instructions and were asked to write down the alphabet, review the descriptions of the traits, and to sort the pictures of fruit and vegetables according to color and size. This ensured again that the preparation material was studied and all had the same sorting-criteria in mind. Additionally, participants were instructed to encode and manipulate the verbal stimuli verbally and to imagine the objects visually in the visual task. For the social task, participants were asked to infer the traits from their contact persons.

To familiarize with the experimental design, nine trials (six task-specific and three order trials) were completed as practice run for each of the tasks and load conditions. In contrast to the main experiment, the participants were provided with feedback in the practice runs, so we could evaluate whether the participants have understood the tasks.

While the participants performed the main experiment on the computer, EEG was recorded from 62 channels (Ag/AgCl scalp ring electrodes; Easycap ®) according to the 10-10 international system. Additionally, electrooculogram (EOG) was recorded from two channels placed at the left outer canthus and above the left eye to control for horizontal and vertical eye movements, respectively. The ground electrode was placed at Fpz. Depending on the

Covid-19 restrictions, the data was referenced either to the tip of the nose or to both ear lobes. As all data was re-referenced to common average later in the preprocessing, the difference in reference should not be noticeable. The signal was recorded at a sampling rate of 1000 Hz and impedances were kept below 10 kΩ .Data acquisition was performed using a 64-channel amplifier (BrainAmp, Brain Products ®). The task was implemented with Presentation ® software (NeuroBehavioral Systems).

After the EEG recordings, participants indicated their strategies to solve the tasks in a survey.

Behavioural data analyses and statistics

The log files from Presentation ® were imported to Excel and descriptive data was extracted. We only used responses that occurred within the 4-s probe period. Reaction times were calculated from the onset of the probe to the response and included correct as well as incorrect responses. Accuracy in percentage was calculated by the number of correct responses divided by the total number of trials and multiplied with 100. Reaction times and accuracy for the tasks and load conditions were calculated without the order trials.

All participants achieved a mean performance over all tasks significantly above chance level in the low (M = 89%, SD = 5.58) and high (M=78%, SD= 6.63) load condition (Mueller-Putz et al., 2008). However, some of the participants indicated after the EEG session that they reversed the given order of manipulation in a task (e.g., sorted the objects from big to small instead of from small to big in the visual task) at a given time point. Thus, we tested whether participants performed significantly below chance in specific blocks. Indeed, six participants reversed the order of a task as they performed significantly below chance level (< 36% for the low load and <13% for the high load condition) in at least one block. Thus, these six participants had to be excluded from behavioral data analysis. As the order of the ranking does not affect brain activity, we did not exclude these participants from the EEG analyses. (Note that these six participants were not “not significantly above chance” and thus might have answered randomly but they were “significantly below chance”, which shows that they participated in the mental ranking during the manipulation condition, only in the wrong order.)

For statistical analyses of the behavioral data, we used IBM SPSS Statistics (version 29). In order to test, whether there is a difference in accuracy and reaction time, we calculated a repeated-measures ANOVA with the within-subject factors task (verbal, social, visual) x load (low and high) and the additional between-subject factor autistic-traits group ($N_{\text{low autistic-traits group}}$ = 48; $N_{\text{high autistic-traits group}}$ =46). Possible violations of the normal distribution should not have an effect on the robustness of the ANOVA (Blanca et al., 2017; Schmider et al., 2010) . Sphericity was confirmed for reaction times, but not for accuracy. Thus, accuracy was Greenhouse-Geisser corrected. Post-hoc tests were performed based on estimated marginal means and Bonferroni-corrected.

EEG data analyses and statistics

EEG preprocessing

The continuous EEG data was preprocessed with BrainVision Analyzer 2.1 (Brain Products ®) to reduce and to control for artifacts as follows: In a visual inspection, large artifacts were removed from the data and if necessary, broken channels were interpolated. Then the data was filtered between 0.1-100 Hz (48 dB/oct) with a notch filter of 50 Hz. The EEG channels

were re-referenced to a common average reference. Then an Independent Component Analysis for ocular correction was applied in order to remove horizontal (saccades) and vertical (blinks) eye movements. Additionally, noise on certain channels could be removed using ICA. Channels that were still too noisy for analyses after ICA were interpolated (in total, one channel was interpolated for 3 participants and 3 channels were interpolated for one participant). Last, the data was again visually inspected and all remaining artifacts were removed. Data of two individuals had to be excluded given that their data quality was still insufficient despite the pre-processing. All analyses were calculated over the remaining 98 participants (49 participants per autistic-traits group). The continuous artifact-free data was then segmented in the 5-s manipulation periods (+/-250 ms). Participants had on average between 29 and 31 manipulation period-trials (SD= 1.8-3.0) per task and load condition.

A priori source space transformation

These segments were then transformed into source space with the build-in module Low-Resolution Electromagnetic Tomography Analysis (LORETA) (Pascual-Marqui et al., 2002, 1994) in BrainVision Analyzer. *A priori* transformation were based on regions of interests (ROIs). Virtual electrodes were placed based on coordinates reported in neuroimaging studies for the social, verbal and visual working memory task (Meyer et al., 2015, 2012; Meyer and Collier, 2020; Todd and Marois, 2004): We defined the Dorsomedial Prefrontal Cortex (DMPFC) as frontal region, its FM-theta phase should modulate posterior gamma amplitude. We furthermore defined 11 posterior regions of interest (ROIs) for the gamma amplitude extraction: left and right Temporal Pole, left and right Temporo-Parietal Junction, left and right Inferior Parietal Lobe, left and right Intraparietal Sulcus, left and right Precuneus / Posterior Cingulate Cortex and the medial Precuneus / Posterior Cingulate Cortex. Please see Table S2 for more information about the ROIs coordinates.

Complex Morlet wavelet transformation

Then complex Morlet wavelet transformation (wavelet normalization: instantaneous amplitude) was applied. For the gamma amplitude, data was filtered between 30-70 Hz in 5 Hz steps with a Morlet parameter of 7. (30 HZ (26-34 Hz gauss), 40 Hz (34-46 Hz), 50 HZ (43-57 Hz), 60 (51-69 Hz), 70 (60-80 HZ). For FM-theta phase (wavelet coefficients, complex values), 5.5 Hz center frequency was filtered with a Morlet parameter of 3.8, thus 4-7 Hz frequency band. These values were transformed to absolute phase values (-pi to +pi) with the *complex data measures solution* module. After gamma amplitude and FM-theta phase extraction, single trials as well as the average over trials of the 5-s manipulation period were exported from Brain Vision Analyzer.

Phase-amplitude coupling

Then, the data was further analyzed in Matlab (R2016a) using in-lab scripts (Berger et al., 2019; Pinal et al., 2015). For the phase-amplitude coupling, only the first 2500 ms of the 5-s manipulation period were analyzed. The reason is that participants indicated that they usually finished their mental ranking in the first half of the manipulation period in the low load condition. The posterior gamma amplitudes were z transformed. The first 2.5-s of all manipulation period-trials were merged. This left us with roughly 375 data points per phase angle for averaging (i.e. roughly 5 theta cycles / s x 2.5 s manipulation stage x 30 trials = 375 data points per phase angle, resulting in over 13000 data points per analyzed phase segment). Then the z-transformed gamma amplitudes were sorted according to FM-theta phase angles and averaged into 10 theta phase segments in order to reduce data complexity. As the values were very small, we multiplied the data by 10 000, so information

was not lost due to rounding decimal places and it was easier to display. See Figure S1 in the supplementary material for detailed information on the phase-amplitude coupling analysis.

Hierarchical generalized regression models

The z-transformed posterior gamma amplitudes sorted according to the FM-theta phase segments were then further investigated by means of hierarchical generalized linear regression analysis conducted in R (version 4.2.2, R Studio 2022.07.1; R Core Team, 2022). Hereby, possible violations of the normal distribution should have little impact on the robustness of regression coefficient estimation (Schmidt and Finan, 2018).

We analyzed regression models for each task and gamma frequency band separately with posterior gamma amplitude as criterion variable and FM-theta phase segments (10 segments), load (low vs. high load), *a priori* defined posterior ROIs (11 ROIs), and autistic-traits groups (low vs. high autistic traits) as predictor variables with random intercepts for each individual. We were predominantly interested in models comprising any interaction between FM-theta phase segments and load, given that we hypothesized that FM-theta phase modulated posterior gamma amplitude depending on load.

The significance of an interaction was determined by comparing the second-order Aikaike information criterion (AICc) value of an interaction model to the AICc value of a model comprising only respective main effect terms. The smaller the AICc value of a model, the more variance of its criterion can be explained by its predictor variables. Thus, a positive difference in AICc values between an interaction and a main effect model indicates that the interaction model explains the criterion variable better than the main effect model. Hereby, a difference of at least 10 implies a large effect (Burnham and Anderson, 2004).

We only analyzed interaction models further that achieved an AICc >10 and if the corresponding main effect models were significant in comparison to a regression model without predictors and with random intercepts for each individual. This ensured that the interaction indeed explained the criterion variable. Otherwise, an interaction model might have been considered as significant given that its model fit was better than the corresponding main effect model – but only because the model fit of the main effect model was very bad.

Thus, we found significant interactions between FM-theta phase segments, load condition and autistic-traits group in specific gamma bands and tasks. As the predictor posterior ROIs did not reach significance in any combination with FM-theta phase, posterior gamma amplitudes were averaged over posterior ROIs for further analyses.

Cosine-model fitting

Then, we investigated whether there was a cosine relationship between the average posterior gamma amplitude and FM-theta phase segments as described in equation 1. Hereby, *Y* refers to individuals' average posterior gamma amplitude, and *X* to their theta phase segment values; and α, β, γ, and δ to free cosine model parameter values denoting the cosine amplitude, frequency shift, phase shift and off-set, respectively. We set β to 1 to prevent an algorithmic solution neglecting our pre-defined theta frequency. Then, α, γ, and δ parameter values were estimated using a Gauss-Newton fitting algorithm.

$$\hat{Y} = \alpha \times cos\big(\beta \times (X + \gamma)\big) + \delta \qquad (1)$$

The model fit to the cosine models was determined by means of the mean absolute error (MAE). It describes the mean absolute deviation between predicted average posterior gamma amplitude values based on cosine model parameter estimates $\hat{y}$ and individuals' actual average posterior gamma amplitude values y for each frontal theta phase segment. The smaller the error, the better the model fit.

In addition to that, we compared the AICc value of the cosine model fit to an intercept model (i.e., the average over all data points – which should be around zero). While positive values already indicated that the cosine model tends to fit better, AICc > 2 indicate that the average posterior gamma amplitude estimates significantly fit to a cosine model and did not just randomly fluctuate around 0 (Burnham and Anderson, 2004).

Last, we determined the most plausible cosine phase-shifts between regression models of differential load and autistic-trait groups. Therefore, we computed the range of most plausible γ estimates by means of two-sided confidence intervals with a significance level of 5%. If 0° was not among the most plausible phase shift values, individuals' gamma amplitude was likely shifted, i.e., significantly different from a null-shift reference model. If 0 was included in the confidence interval, the highest gamma amplitude was locked in the trough of FM-theta (i.e., 180°) as in the null-sift reference model.

Circular-linear correlations

Circular-linear correlations between the phase segment of FM-theta with the highest gamma amplitude (i.e., preferred phase segment) and AQ scores of the subscales over all participants as well as performance were computed (Berens, 2009; Pinal et al., 2015). These correlations were only calculated for the tasks and frequency bands showing a significant phase-amplitude coupling.

REFERENCES

Anticevic, A., Repovs, G., Shulman, G.L., Barch, D.M., 2010. When less is more: TPJ and default network deactivation during encoding predicts working memory performance. Neuroimage 49, 2638–2648. https://doi.org/10.1016/j.neuroimage.2009.11.008

Audrain, S.P., Urbain, C.M., Yuk, V., Leung, R.C., Wong, S.M., Taylor, M.J., 2020. Frequency-specific neural synchrony in autism during memory encoding, maintenance and recognition. Brain Commun. 2, 1–15. https://doi.org/10.1093/braincomms/fcaa094

Baddeley, A., 2003. Working memory: Looking back and looking forward. Nat. Rev. Neurosci. 4, 829–839. https://doi.org/10.1038/nrn1201

Baddeley, A.D., Allen, R.J., Hitch, G.J., 2011. Binding in visual working memory: The role of the episodic buffer. Neuropsychologia 49, 1393–1400. https://doi.org/10.1016/j.neuropsychologia.2010.12.042

Barbey, A.K., Koenigs, N., Grafman, J., 2013. Dorsolateral Prefrontal Contributions to Human Working Memory. Cortex 49, 1195–1205. https://doi.org/10.1016/j.cortex.2012.05.022.Dorsolateral

Barendse, E.M., Hendriks, M.P., Jansen, J.F., Backes, W.H., Hofman, P.A., Thoonen, G., Kessels, R.P., Aldenkamp, A.P., 2013. Working memory deficits in high-functioning adolescents with autism spectrum disorders: neuropsychological and neuroimaging correlates. J. Neurodev. Disord. 5, 14. https://doi.org/10.1186/1866-1955-5-14

Barendse, E.M., Schreuder, L.J., Thoonen, G., Hendriks, M.P.H., Kessels, R.P.C., Backes, W.H., Aldenkamp, A.P., Jansen, J.F.A., 2018. Working memory network alterations in high-functioning adolescents with an autism spectrum disorder. Psychiatry Clin. Neurosci. 72, 73–83. https://doi.org/10.1111/pcn.12602

Baron-Cohen, S., Wheelwright, S., Skinner, R., Martin, J., Clubley, E., 2001. The Autism Spectrum Quotient : Evidence from Asperger syndrome/high functioning autism, males and females, scientists and mathematicians. J. Autism Dev. Disord. 31, 5–17. https://doi.org/10.1023/A:1005653411471

Berens, P., 2009. CircStat : A MATLAB Toolbox for Circular Statistics. J. Stat. Softw. 31, 1–21. https://doi.org/10.18637/jss.v031.i10

Berger, B., Griesmayr, B., Minarik, T., Biel, A.L., Pinal, D., Sterr, A., Sauseng, P., 2019. Dynamic regulation of interregional cortical communication by slow brain oscillations during working memory. Nat. Commun. 10, 1–12. https://doi.org/10.1038/s41467-019-12057-0

Blanca, M.J., Alarcón, R., Arnau, J., Bono, R., Bendayan, R., 2017. Non-normal data: Is ANOVA still a valid option? Psicothema 29, 552–557. https://doi.org/10.7334/psicothema2016.383

Braver, T.S., Cohen, J.D., Nystrom, L.E., Jonides, J., Smith, E., Noll, D.C., 1997. A Parametric Study of Prefrontal Cortex Involvement in Human Working Memory. Neuroimage 5, 49–62.

Buckner, R.L., Andrews-Hanna, J.R., Schacter, D.L., 2008. The brain's default network: Anatomy, function, and relevance to disease. Ann. N. Y. Acad. Sci. 1124, 1–38. https://doi.org/10.1196/annals.1440.011

Burnham, K.P., Anderson, D.R., 2004. Multimodel inference: Understanding AIC and BIC in model selection. Sociol. Methods Res. 33, 261–304. https://doi.org/10.1177/0049124104268644

Campbell, J.I.D., Thompson, V.A., 2012. MorePower 6.0 for ANOVA with relational confidence intervals and Bayesian analysis. Behav. Res. Methods 44, 1255–1265. https://doi.org/10.3758/s13428-012-0186-0

Cattell, R., Cattell, A., 1960. Handbook for the individual or group culture fair intelligence test. Savoy, Inst. Personal. Abil. Test.

Cavanagh, J.F., Frank, M.J., 2014. Frontal theta as a mechanism for cognitive control. Trends Cogn. Sci. 18, 414–421. https://doi.org/10.1016/j.tics.2014.04.012

Cohen, M.X., 2014. A neural microcircuit for cognitive conflict detection and signaling. Trends Neurosci. 37, 480–490. https://doi.org/10.1016/j.tins.2014.06.004

Cowan, N., 2008. What are the differences between long-term, short-term, and working

memory? Prog Brain Res. 169, 323–338. https://doi.org/10.1016/S0079-6123(07)00020-9.What
D'Esposito, M., 2007. From cognitive to neural models of working memory. Philos. Trans. R. Soc. B Biol. Sci. 362, 761–772. https://doi.org/10.1098/rstb.2007.2086
de Vries, I.E.J., Slagter, H.A., Olivers, C.N.L., 2020. Oscillatory Control over Representational States in Working Memory. Trends Cogn. Sci. 24, 150–162. https://doi.org/10.1016/j.tics.2019.11.006
Dichter, G.S., 2012. Functional magnetic resonance imaging of autism spectrum disorders. Dialogues Clin. Neurosci. 14, 319–351.
Dumas, J.E., Johnson, M., Lynch, A.M., 2002. Likableness, familiarity, and frequency of 844 person-descriptive words. Pers. Individ. Dif. 32, 523–531. https://doi.org/10.1016/S0191-8869(01)00054-X
Emch, M., von Bastian, C.C., Koch, K., 2019. Neural correlates of verbal working memory: An fMRI meta-analysis. Front. Hum. Neurosci. 13, 1–17. https://doi.org/10.3389/fnhum.2019.00180
Ferrari, C., Vecchi, T., Todorov, A., Cattaneo, Z., 2016. Interfering with activity in the dorsomedial prefrontal cortex via TMS affects social impressions updating. Cogn. Affect. Behav. Neurosci. 16, 626–634. https://doi.org/10.3758/s13415-016-0419-2
Fox, M.D., Snyder, A.Z., Vincent, J.L., Corbetta, M., Van Essen, D.C., Raichle, M.E., 2005. The human brain is intrinsically organized into dynamic, anticorrelated functional networks. Proc. Natl. Acad. Sci. U. S. A. 102, 9673–8. https://doi.org/10.1073/pnas.0504136102
Freitag, C.M., Retz-Junginger, P., Retz, W., Seitz, C., Palmason, H., Meyer, J., Rösler, M., Von Gontard, A., 2007. Evaluation der deutschen Version des Autismus-Spektrum-Quotienten (AQ) - Die kurzversion AQ-k. Z. Klin. Psychol. Psychother. 36, 280–289. https://doi.org/10.1026/1616-3443.36.4.280
Frith, C.D., Frith, U., 2006. The Neural Basis of Mentalizing. Neuron 50, 531–534. https://doi.org/10.1016/j.neuron.2006.05.001
Fusar-Poli, P., Salazar de Pablo, G., De Micheli, A., Nieman, D.H., Correll, C.U., Kessing, L.V., Pfennig, A., Bechdolf, A., Borgwardt, S., Arango, C., van Amelsvoort, T., 2020. What is good mental health? A scoping review. Eur. Neuropsychopharmacol. 31, 33–46. https://doi.org/10.1016/j.euroneuro.2019.12.105
Gebauer, L., Foster, N.E.V., Vuust, P., Hyde, K.L., 2015. Is there a bit of autism in all of us? Autism spectrum traits are related to cortical thickness differences in both autism and typical development. Res. Autism Spectr. Disord. 13–14, 8–14. https://doi.org/10.1016/j.rasd.2014.12.013
Griesmayr, B., Berger, B., Stelzig-Schoeler, R., Aichhorn, W., Bergmann, J., Sauseng, P., 2014. EEG theta phase coupling during executive control of visual working memory investigated in individuals with schizophrenia and in healthy controls. Cogn. Affect. Behav. Neurosci. 14, 1340–1355. https://doi.org/10.3758/s13415-014-0272-0
Grühn, D., Smith, J., 2008. Characteristics for 200 words rated by young and older adults: Age-dependent evaluations of German adjectives (AGE). Behav. Res. Methods 40, 1088–1097. https://doi.org/10.3758/BRM.40.4.1088
Hamilton, A., Marsh, L., 2013. Two systems for action comprehension in autism: Mirroring and mentalizing, in: Baron-Cohen, Tager-Flusberg, Lombardo (Eds.), Understanding Other Minds: Perspectives from Developmental Social Neuroscience. pp. 380–396. https://doi.org/10.1093/acprof:oso/9780199692972
Hill, A.T., Van Der Elst, J., Bigelow, F.J., Lum, J.A.G., Enticott, P.G., 2022. Right anterior theta connectivity predicts autistic social traits in typically developing children. Biol. Psychol. 175, 108448. https://doi.org/10.1016/j.biopsycho.2022.108448
Honkanen, R., Rouhinen, S., Wang, S.H., Palva, J.M., Palva, S., 2015. Gamma oscillations underlie the maintenance of feature-specific information and the contents of visual working memory. Cereb. Cortex 25, 3788–3801. https://doi.org/10.1093/cercor/bhu263
Isaksson, J., Van't Westeinde, A., Cauvet, Kuja-Halkola, R., Lundin, K., Neufeld, J., Willfors, C., Bölte, S., 2019. Social Cognition in Autism and Other Neurodevelopmental Disorders: A Co-twin Control Study. J. Autism Dev. Disord. 49, 2838–2848.

https://doi.org/10.1007/s10803-019-04001-4
Just, M.A., Keller, T.A., Malave, V.L., Kana, R.K., Varma, S., 2012. Autism as a neural systems disorder. Neurosci. Biobehav. Rev. 36, 1292–1313. https://doi.org/10.1016/j.neubiorev.2012.02.007.Autism
Koshino, H., Kana, R.K., Keller, T.A., Cherkassky, V.L., Minshew, N.J., Just, M.A., 2008. fMRI Investigation of Working Memory for Faces in Autism: Visual Coding and Underconnectivity with Frontal Areas. Cerebal Cortex 18, 289–300. https://doi.org/10.1093/cercor/bhm054.fMRI
Larrain-Valenzuela, J., Zamorano, F., Soto-Icaza, P., Carrasco, X., Herrera, C., Daiber, F., Aboitiz, F., Billeke, P., 2017. Theta and Alpha Oscillation Impairments in Autistic Spectrum Disorder Reflect Working Memory Deficit. Sci. Rep. 7, 1–11. https://doi.org/10.1038/s41598-017-14744-8
Lau, W.Y.P., Peterson, C.C., Attwood, T., Garnett, M.S., Kelly, A.B., 2016. Parents on the autism continuum: Links with parenting efficacy. Res. Autism Spectr. Disord. 26, 57–64. https://doi.org/10.1016/j.rasd.2016.02.007
Lehrl, S., Triebig, G., Fischer, B., 1995. Multiple choice vocabulary test MWT as a valid and short test to estimate premorbid intelligence. Acta Neurol. Scand. 91, 335–345. https://doi.org/10.1111/j.1600-0404.1995.tb07018.x
Mealey, A., Abbott, G., Byrne, L.K., McGillivray, J., 2014. Overlap between autistic and schizotypal personality traits is not accounted for by anxiety and depression. Psychiatry Res. 219, 380–385. https://doi.org/10.1016/j.psychres.2014.05.040
Meyer, M.L., Collier, E., 2020. Theory of minds: Managing mental state inferences in working memory is associated with the dorsomedial subsystem of the default network and social integration. Soc. Cogn. Affect. Neurosci. 15, 63–73. https://doi.org/10.1093/scan/nsaa022
Meyer, M.L., Lieberman, M.D., 2016. Social Working Memory Training Improves Perspective-Taking Accuracy. Soc. Psychol. Personal. Sci. 7, 381–389. https://doi.org/10.1177/1948550615624143
Meyer, M.L., Lieberman, M.D., 2012. Social working memory: Neurocognitive networks and directions for future research. Front. Psychol. 3, 1–11. https://doi.org/10.3389/fpsyg.2012.00571
Meyer, M.L., Spunt, R.P., Berkman, E.T., Taylor, S.E., Lieberman, M.D., 2012. Evidence for social working memory from a parametric functional MRI study. Proc. Natl. Acad. Sci. 109, 1883–1888. https://doi.org/10.1073/pnas.1121077109
Meyer, M.L., Taylor, S.E., Lieberman, M.D., 2015. Social working memory and its distinctive link to social cognitive ability: An fMRI study. Soc. Cogn. Affect. Neurosci. 10, 1338–1347. https://doi.org/10.1093/scan/nsv065
Miller, E.K., Lundqvist, M., Bastos, A.M., 2018. Working Memory 2.0. Neuron 100, 463–475. https://doi.org/10.1016/j.neuron.2018.09.023
Mottaghy, F.M., Gangitano, M., Sparing, R., Krause, B.J., Pascual-Leone, A., 2002. Segregation of Areas Related to Visual Working Memory in the Prefrontal Cortex Revealed by rTMS. Cereb. Cortex 12, 369–375. https://doi.org/10.1093/cercor/12.4.369
Mueller-Putz, G., Scherer, R., Brunner, C., Leeb, R., Pfurtscheller, G., 2008. Better than random: A closer look on BCI results. Int. J. Bioelectromagn. 10, 52–55.
Mull, B.R., Seyal, M., 2001. Transcranial magnetic stimulation of left prefrontal cortex impairs working memory. Clin Neurophysiol 112, 1672–1675. https://doi.org/S1388-2457(01)00606-X [pii]
O'Reilly, C., Lewis, J.D., Elsabbagh, M., 2017. Is functional brain connectivity atypical in autism? A systematic review of EEG and MEG studies. PLoS One 12, 1–28. https://doi.org/10.1371/journal.pone.0175870
Oldfield, R.C., 1971. The assessment and analysis ofhandedness: The Edinburgh inventory. Neuropsychologia 9, 97–113.
Osaka, N., Otsuka, Y., Hirose, N., Ikeda, T., Mima, T., Fukuyama, H., Osaka, M., 2007. Transcranial magnetic stimulation (TMS) applied to left dorsolateral prefrontal cortex disrupts verbal working memory performance in humans. Neurosci. Lett. 418, 232–235. https://doi.org/10.1016/j.neulet.2007.01.087

Owen, A.M., McMillan, K.M., Laird, A.R., Bullmore, E., 2005. N-back working memory paradigm: A meta-analysis of normative functional neuroimaging studies. Hum. Brain Mapp. 25, 46–59. https://doi.org/10.1002/hbm.20131
Palva, J.M., Monto, S., Kulashekhar, S., Palva, S., 2010. Neuronal synchrony reveals working memory networks and predicts individual memory capacity. Proc. Natl. Acad. Sci. U. S. A. 107, 7580–7585. https://doi.org/10.1073/pnas.0913113107
Pascual-Marqui, R.D., Esslen, M., Kochi, K., Lehmann, D., 2002. Functional imaging with low-resolution brain electromagnetic tomography (LORETA): A review. Methods Find. Exp. Clin. Pharmacol. 24, 91–95.
Pascual-Marqui, R.D., Michel, C.M., Lehmann, D., 1994. Low resolution electromagnetic tomography: a new method for localizing electrical activity in the brain. Int. J. Psychophysiol. 18, 49–65.
Pearson, J., 2019. The human imagination: the cognitive neuroscience of visual mental imagery. Nat. Rev. Neurosci. 20, 624–634. https://doi.org/10.1038/s41583-019-0202-9
Pinal, D., Zurrón, M., Díaz, F., Sauseng, P., 2015. Stuck in default mode: Inefficient cross-frequency synchronization may lead to age-related short-term memory decline. Neurobiol. Aging 36, 1611–1618. https://doi.org/10.1016/j.neurobiolaging.2015.01.009
R Core Team, N. a., 2022. R: A Language and Environment for Statistical Computing. Vienna, Austria. URL https//www.R-project.org.
Rahko, J.S., Vuontela, V.A., Carlson, S., Nikkinen, J., Hurtig, T.M., Kuusikko-Gauffin, S., Mattila, M.L., Jussila, K.K., Remes, J.J., Jansson-Verkasalo, E.M., Aronen, E.T., Pauls, D.L., Ebeling, H.E., Tervonen, O., Moilanen, I.K., Kiviniemi, V.J., 2016. Attention and Working Memory in Adolescents with Autism Spectrum Disorder: A Functional MRI Study. Child Psychiatry Hum. Dev. 47, 503–517. https://doi.org/10.1007/s10578-015-0583-6
Rammstedt, B., John, O.P., 2005. Kurzversion des Big Five Inventory (BFI-K): Entwicklung und validierung eines ökonomischen inventars zur erfassung der fünf faktoren der persönlichkeit. Diagnostica 51, 195–206. https://doi.org/10.1026/0012-1924.51.4.195
Ratcliffe, O., Shapiro, K., Staresina, B.P., 2022. Fronto-medial theta coordinates posterior maintenance of working memory content. Curr. Biol. 32, 2121-2129.e3. https://doi.org/10.1016/j.cub.2022.03.045
Richmond, L.L., Thorpe, M., Berryhill, M.E., Klugman, J., Olson, I.R., 2013. Individual Differences in Autistic Trait Load in the General Population Predicts Visual Working Memory Performance. Q. J. Exp. Psychol. 66, 1182–1195. https://doi.org/https://doi.org/10.1080/17470218.2012.734831
Sauseng, P., Tschentscher, N., Biel, A.L., 2019. Be Prepared: Tune to FM-Theta for Cognitive Control. Trends Neurosci. 42, 307–309. https://doi.org/10.1016/j.tins.2019.02.006
Schmider, E., Ziegler, M., Danay, E., Beyer, L., Bühner, M., 2010. Is It Really Robust?: Reinvestigating the robustness of ANOVA against violations of the normal distribution assumption. Methodology 6, 147–151. https://doi.org/10.1027/1614-2241/a000016
Schmidt, A.F., Finan, C., 2018. Linear regression and the normality assumption. J. Clin. Epidemiol. 98, 146–151. https://doi.org/10.1016/j.jclinepi.2017.12.006
Schurz, M., Radua, J., Aichhorn, M., Richlan, F., Perner, J., 2014. Fractionating theory of mind: A meta-analysis of functional brain imaging studies. Neurosci. Biobehav. Rev. 42, 9–34. https://doi.org/10.1016/j.neubiorev.2014.01.009
Schurz, M., Radua, J., Tholen, M.G., Maliske, L., Margulies, D.S., Mars, R.B., Sallet, J., Kanske, P., 2021. Toward a hierarchical model of social cognition: A neuroimaging meta-analysis and integrative review of empathy and theory of mind. Psychol. Bull. 147, 293–327. https://doi.org/10.1037/bul0000303
Sevgi, M., Diaconescu, A.O., Tittgemeyer, M., Schilbach, L., 2016. Social Bayes: Using Bayesian Modeling to Study Autistic Trait–Related Differences in Social Cognition. Biol. Psychiatry 80, 112–119. https://doi.org/10.1016/j.biopsych.2015.11.025
Smith, R., Lane, R.D., Alkozei, A., Bao, J., Smith, C., Sanova, A., Nettles, M., Killgore, W.D.S., 2017. Maintaining the feelings of others in working memory is associated with activation of the left anterior insula and left frontal-parietal control network. Soc. Cogn.

Affect. Neurosci. 12, 848–860. https://doi.org/10.1093/scan/nsx011
Spunt, R.P., Lieberman, M.D., 2013. The Busy Social Brain: Evidence for Automaticity and Control in the Neural Systems Supporting Social Cognition and Action Understanding. Psychol. Sci. 24, 80–86. https://doi.org/10.1177/0956797612450884
Sumiyoshi, C., Kawakubo, Y., Suga, M., Sumiyoshi, T., Kasai, K., 2011. Impaired ability to organize information in individuals with autism spectrum disorders and their siblings. Neurosci. Res. 69, 252–257. https://doi.org/10.1016/j.neures.2010.11.007
Todd, J.J., Marois, R., 2004. Capacity limit of visual short-term memory in human posterior parietal cortex. Nature 428, 751–754. https://doi.org/10.1038/nature02466
Urbain, C.M., Pang, E.W., Taylor, M.J., 2015. Atypical spatiotemporal signatures of working memory brain processes in autism. Transl. Psychiatry 5, e617-9. https://doi.org/10.1038/tp.2015.107
Van Overwalle, F., 2011. A dissociation between social mentalizing and general reasoning. Neuroimage 54, 1589–1599. https://doi.org/10.1016/j.neuroimage.2010.09.043
Van Overwalle, F., 2009. Social cognition and the brain: A meta-analysis. Hum. Brain Mapp. 30, 829–858. https://doi.org/10.1002/hbm.20547
Velikonja, T., Fett, A.K., Velthorst, E., 2019. Patterns of Nonsocial and Social Cognitive Functioning in Adults with Autism Spectrum Disorder: A Systematic Review and Meta-analysis. JAMA Psychiatry 76, 135–151. https://doi.org/10.1001/jamapsychiatry.2018.3645
Vogan, V.M., Francis, K.E., Morgan, B.R., Smith, M. Lou, Taylor, M.J., 2018. Load matters: Neural correlates of verbal working memory in children with autism spectrum disorder. J. Neurodev. Disord. 10, 1–12. https://doi.org/10.1186/s11689-018-9236-y
Vogan, V.M., Morgan, B.R., Lee, W., Powell, T.L., Smith, M. Lou, Taylor, M.J., 2014. The neural correlates of visuo-spatial working memory in children with autism spectrum disorder: effects of cognitive load. J. Neurodev. Disord. 6, 1–15.
Vogan, V.M., Morgan, B.R., Smith, M. Lou, Taylor, M.J., 2019. Functional changes during visuo-spatial working memory in autism spectrum disorder: 2-year longitudinal functional magnetic resonance imaging study. Autism 23, 639–652. https://doi.org/10.1177/1362361318766572
Wang, Y., Zhang, Y. bing, Liu, L. lu, Cui, J. fang, Wang, J., Shum, D.H.K., van Amelsvoort, T., Chan, R.C.K., 2017. A Meta-Analysis of Working Memory Impairments in Autism Spectrum Disorders. Neuropsychol. Rev. 27, 46–61. https://doi.org/10.1007/s11065-016-9336-y
Williams, D.L., Goldstein, G., Carpenter, P.A., Minshew, N.J., 2005. Verbal and spatial working memory in autism. J. Autism Dev. Disord. 35, 747–756. https://doi.org/10.1007/s10803-005-0021-x
Williams, D.M., Jarrold, C., Grainger, C., Lind, S.E., 2014. Diminished time-based, but undiminished event-based, prospective memory among intellectually high-functioning adults with autism spectrum disorder: Relation to working memory ability. Neuropsychology 28, 30–42. https://doi.org/10.1037/neu0000008
Wimmer, H., Perner, J., 1983. Beliefs about beliefs: Representation and constraircing function of wrong bekfs in young children's understanding of deception. Cognition 13, 103–128. https://doi.org/10.1016/0010-0277(83)90004-5
Xie, R., Sun, X., Yang, L., Guo, Y., 2020. Characteristic Executive Dysfunction for High-Functioning Autism Sustained to Adulthood. Autism Res. 13, 2102–2121. https://doi.org/10.1002/aur.2304
Yuk, V., Urbain, C., Anagnostou, E., Taylor, M.J., 2020. Frontoparietal Network Connectivity During an N-Back Task in Adults With Autism Spectrum Disorder. Front. Psychiatry 11, 1–16. https://doi.org/10.3389/fpsyt.2020.551808